An Uncertainty-Informed Machine Learning Framework for Predicting Fire Damage to Cables and Cabinets in Switchgear Rooms

Van Tuan Ho [a], Saerin Lim[b], Seoung Bum Kim[b], Weon Gyu Shin [a*]
[a]Department of Mechanical Engineering, Chungnam National University, Daejeon 34134, Republic of Korea
[b]School of Industrial and Management Engineering, Korea University, Seoul, 02841, Republic of Korea
[*]*Corresponding author: wgshin@cnu.ac.kr (W. G. Shin)*

Keywords : Nuclear power plants (NPPs), Switchgear room (SWGR), Machine Learning (ML), Uncertainty quantification (UQ), CFAST.

1. Introduction

Nuclear power plants (NPPs) are critical infrastructure that require stringent safety measures to ensure reliable and continuous electricity generation. The switchgear room (SWGR) contains cable trays and electrical cabinets responsible for supplying and distributing power to essential systems. Consequently, a fire within the SWGR can pose a significant threat to NPP safety, especially without effective fire protection measures. Yu Zhang et al. [1] investigated the effects of room dimensions, ambient temperature, and air changes per hour on the cable and cabinet damage in a SWGR. However, their study did not consider the effects of the spatial positions and fire locations of cables and cabinets.

Machine learning (ML) has increasingly been applied to fire safety research as an efficient alternative to computationally intensive CFD simulations. Singh et al. [2] developed a multilayer neural network using 11,340 CFAST simulation cases, achieving an R^2 value of 0.9965. However, high predictive accuracy alone does not provide sufficient insight into model interpretability, prediction plausibility, or feature contributions, posing challenges to the deployment of ML models in safety-critical environments. To address this gap, Heo et al. [3] employed Shapley Additive Explanations (SHAP) to improve interpretability by revealing the relationships between input features and predictions. However, model interpretability and high predictive accuracy are not sufficient to establish the reliability of ML models for safety-critical applications. In NPPs, inadequately validated or unreliable uncertainty estimates may induce unwarranted confidence in predictions, reducing the effectiveness of risk-informed decisions and non-conservative safety margins. Therefore, uncertainty quantification is important for evaluating prediction confidence and ensuring the reliability of predictions.

This study develops a surrogate-based framework for efficiently evaluating fire safety risks in NPP switchgear rooms. First, we conduct an sensitivity analysis to analyze the influence of fire positions, cabinet and cable locations, ambient temperatures, and air changes per hour (ACH) on damage to cabinet and cables. Second, an ML-based surrogate model was developed, incorporating SHAP analysis to interpret the predictions and assess feature contributions. Third, uncertainty thresholds were determined based on relative error criteria, providing reliability-based threshold to differentiate reliable predictions from cases that necessitate CFD simulations.

2. Methods

2.1 Overview of Switchgear room

Fig. 1 presents the geometry of the SWGR, with cabinets and cables represented as points to simplify the model. Cabinet 1 is designated as the fire source, with fire growth following a t^2 profile. The heat release rate (HRR) increases to a peak of 464 kW at 12 min, remains constant for the next 8 min, and then decreases linearly to zero after 20 min.

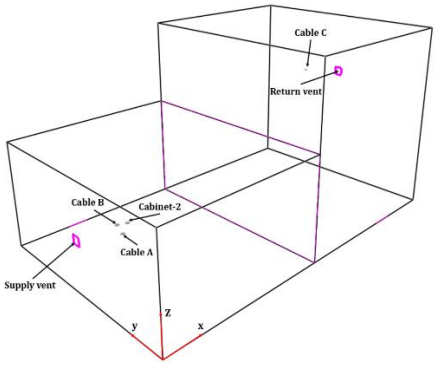


Fig. 1. CFAST model geometry of the SWGR

2.2 Data generation and Data pre-processing

In total, 6,400 CFAST simulation cases were collected by systematically varying the fire positions, cabinet and cable positions, ambient temperatures, and air changes per hour (ACH). As shown in Table 1, Cabinet and cable damage times were identified from the CFAST outputs according to the following criteria [4]: (a) incident heat flux exceeding 6 kW/m² and (b) surface temperature of 205°C.

Table 1: Summary of undamaged and damaged cases

Component	Undamaged	Damaged	Total
Cable A	0	6.400	6.400
Cable B	587	5.813	
Cable C	6.400	0	

Cabinet 2	328	6.072	

2.3 Overview of machine learning framework

Fig. 2 presents the overall machine learning framework used in this study, consisting of five steps: data generation, data splitting, model development, hyperparameter optimization, and comprehensive evaluation.

In this study, epistemic uncertainty was quantified using the bootstrap aggregating (bagging) approach [5]. The original dataset was resampled with replacement to construct multiple training datasets, with a ML model trained on each resampled dataset. For each input, the final prediction was obtained by aggregating the outputs. Epistemic uncertainty is reflected by the dispersion of predictions, such that a larger spread indicates less confidence in the model.

The relative error (RE) was used to quantify prediction deviations and distinguish between high- and low-risk predictions. Because no universally accepted RE threshold has been established for fire prediction, three representative thresholds of 3%, 5%, and 10% were evaluated. To define an uncertainty threshold (σ*) for selecting cases for CFD simulation, a binary classification was used, with high-risk cases identified based on whether RE values exceeded the specified criterion. False Positive Rate (FPR) [6] quantified unnecessary CFD simulations while Recall [6] measured high-risk detection.

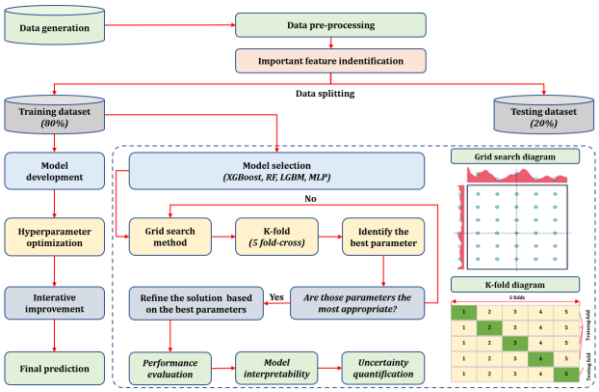


Fig. 2. The framework of the machine learning

3. Results

3.1 Sensitivity analysis

3.1.1 The effects of Cable A, Cable B, and fire source locations

Fig. 3(a-b) illustrates the Cable A damage time with the Z-axis positions of Cable A and Cable B at AX = 2.3 m and the fire at AX = 2.7 m, respectively. The results show that Cable A's heat-flux damage time becomes longer at higher positions due to its distance from the fire source, whereas it decreases at lower fire locations as the fire source approaches Cable A. In contrast, the damage time based on surface temperature exhibits a non-monotonic pattern. The damage time increases with distance from the fire source at AZ = 2.5-2.6 m, whereas damage time decreases as the cable approaches the ceiling hot gas layer at AZ = 2.7-2.8 m. Similarly, at FZ = 2.2-2.4 m, damage time decreases as fire source approaches Cable A, while at FZ = 2.1 m, earlier damage is attributed to the thicker ceiling hot-gas layer formed near Cable A.

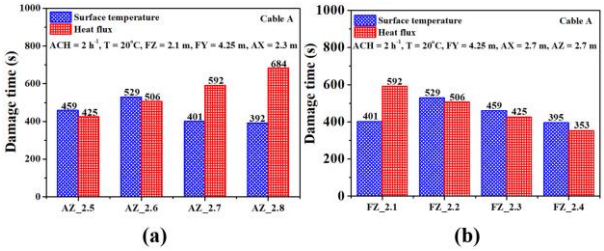


Fig. 3. Variation in Cable A damage time with the Z-axis positions of (a) Cable A and Cable B at AX = 2.3 m, (b) the fire source at AX = 2.7 m

3.1.2 The influence of ACH variation

Fig. 4(a-b) presents the damage times of Cable A, Cable B, and Cabinet 2 across different ACH. The results indicate that variations in ACH have a negligible influence on the damage time of Cable A due to its proximity to the fire. The damage time of Cabinet 2 and Cable B reduces at higher ACH. This trend is attributed to faster hot-gas transport to the downstream components (Cabinet 2 and Cable B) at higher ACH, which enhances convective heat transfer.

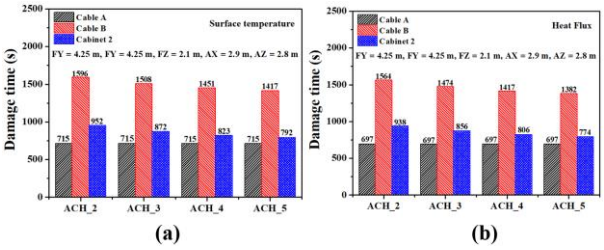


Fig. 4. Damage time of Cable A, Cable B, and Cabinet 2: (a) Surface temperature, (b) Heat flux

3.2 Machine learning performance

3.2.1 Predictive accuracy

Table 2 presents the predictive accuracy of the ML models. MLP provides the highest prediction accuracy for Cable A while LGBM achieves the best performance for Cabinet 2 and Cable B. Fig. 5 shows the LGBM predictions for the testing datasets, demonstrating close agreement between predicted and simulated damage times for the cables and cabinet.

Table 2: Comparative performance of ML models

Cable bundle	Error metric	LGBM	XGBoost	MLP	RF
Cable A	R^2	0.987	0.982	**0.988**	0.962
	MAE	7.73	8.26	**6.42**	16.09
	MAPE	2.18%	2.10%	**1.88%**	4.00%
	RMSE	13.56	15.89	**11.83**	22.99
Cable B	R^2	**0.998**	0.998	0.997	0.995
	MAE	**5.91**	7.21	12.97	15.32
	MAPE	**0.79%**	1.07%	2.46%	2.44%
	RMSE	**16.44**	18.12	21.51	26.48
Cabinet 2	R^2	0.995	**0.996**	0.968	0.947
	MAE	**1.99**	2.55	7.77	7.44
	MAPE	**0.28%**	0.38%	1.16%	1.06%
	RMSE	5.28	**4.84**	14.86	19.16

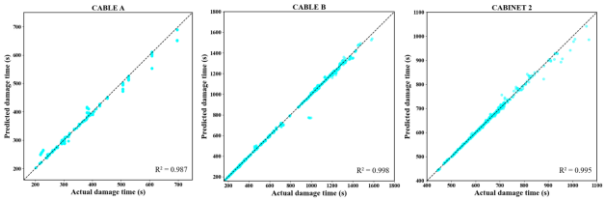


Fig. 5. The predictive outcomes of the LGBM model

3.2.2 SHAP interpretation

Fig. 6(a-c) shows SHAP-based feature contribution analysis for Cable A, Cable B, and Cabinet 2, respectively. The results show that FZ, AX, and FZ are the most influential features for predicting the damage times of Cable A, Cable B, and Cabinet 2, respectively. The SHAP analysis shows that high FZ values reduce the predicted damage time for Cabinet 2 and Cable A as the fire source moves closer, whereas lower FZ values increase it. However, at positive SHAP values for Cable A, lower FZ may also cause earlier damage due to a thicker hot-gas layer near the cables. For Cable B, small AX values reduce damage time because of its proximity to Cable A, while high AX values increase it. These trends align with the sensitivity analysis.

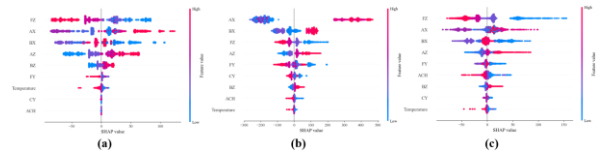


Fig. 6. SHAP-based feature contribution analysis for the LGBM model: (a) Cable A, (b) Cable B, and (c) Cabinet 2

3.2.3 Uncertainty analysis

Table 3 presents optimized uncertainty thresholds and classification results across RE thresholds. High-risk cases were reliably detected by the framework, yielding recall values greater than 95.3% for all cabinets and cables, with perfect recall for Cable B and Cabinet 2 at the 5% RE threshold. As shown in Fig. 7, the scatter plots indicate higher uncertainty corresponds to an increased tendency for prediction errors to exceed the 5% error criterion. Moreover, increasing the RE criterion from 3% to 10% generally reduced the FPR. For example, Cable A decreased from 0.21 to 0.02. Cabinet 2 exhibited the lowest FPR of 0.002 at 5% RE, indicating minimal unnecessary CFD simulations. Overall, the framework provides an efficient decision-support tool by flagging high-uncertainty predictions for further verification while allowing reliable low-uncertainty predictions to be used directly.

Table 3: Optimized uncertainty thresholds and classification performance under RE thresholds

Cable bundle	RE =3%			RE = 5%			RE = 10%		
	σ*	FPR	Recall	σ*	FPR	Recall	σ*	FPR	Recall
Cable A	3.77	0.21	0.953	4.41	0.15	0.954	16.2	0.02	0.968
Cable B	4.64	0.29	0.964	10.38	0.07	1.0	10.38	0.07	1.0
Cabinet 2	8.87	0.02	1.0	22.51	0.002	1.0	-	-	-

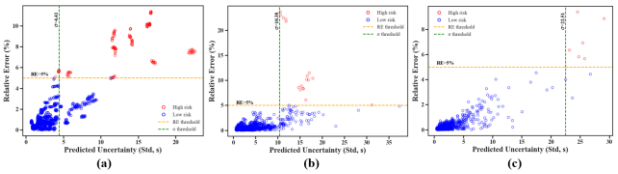


Fig. 7. Uncertainty threshold for risk classification at RE criterion of 5% of the LGBM model: (a) Cable A, (b) Cable B, and (c) Cabinet 2

4. Conclusions

1. **The effects of Cable A, Cable B, and fire source locations:** Heat-flux damage time increases with higher Cable A and lower fire locations, whereas damage based on surface-temperature is a non-monotonic trend because of the hot-gas layer, highlighting its critical role in cable damage.
2. **The influence of ACH variation:** The influence of ACH is negligible for cables and the cabinet positioned near the fire source. Higher ACH can accelerate damage to downstream components by enhancing hot-gas transport.
3. **Machine learning performance:** The ML models provided accurate damage-time predictions that closely agreed with the actual values. The SHAP analysis were consistent with the sensitivity analysis, revealing physically meaningful effects of the primary factors influencing damage. High-risk predictions were reliably detected through uncertainty quantification, yielding recall values above 95.3% across all cables and the cabinet. Overall, the ML framework enables rapid and reliable fire-damage predictions, enabling efficient risk assessment, scenario assessment, and sensitivity analysis without requiring repeated computationally intensive CFD simulations in nuclear power plants.

REFERENCES

[1] Y. Zhang, S. Lim, J. Heo, J. Bae, S. B. Kim, and W.

G. Shin, CFAST Simulations and Application of a Machine Learning Algorithm for the Fire Safety of a Switchgear Room, Nuclear Engineering and Technology, p. 104006, 2025.
[2] S. K. Singh, J. Bae, Y. Zhang, S. Lim, J. Heo, S. B. Kim, and W. G. Shin, Identification of Primary Input Parameters Affecting Evacuation in Ventilated Main Control Room through CFAST Simulations and Application of a Machine Learning Algorithm to Replace CFAST Model, Nuclear Engineering and Technology, Vol. 56, No. 9, pp. 3717–3729, 2024.
[3] J. Heo, Y. Zhang, J. Bae, S. Lim, W. G. Shin, and S. B. Kim, Explainable Machine Learning-Based Meta-M odeling for Predicting Fire Damage to Motor Control C abinets in a Switchgear Room, Nuclear Engineering and Technology, p. 103862, 2025.
[4] Fire Dynamics Tools (FDTs) Quantitative Fire Hazard Analysis Methods for the U.S. Nuclear Regulatory Commission Fire Protection Inspection Program (NUREG-1805, Final Report).
[5] B. Efron, Bootstrap methods: another look at the jackknife, Breakthroughs in Statistics: Methodology and Distribution, Springer, New York, NY, 1992.
[6] T. Fawcett, An Introduction to ROC Analysis, Pattern Recognition Letters, 27(8), pp. 861–874, 2006.